15N NMR study of nitrate ion structure and dynamics in hydrotalcite-like compounds

Article *in* American Mineralogist · January 2000

DOI: 10.2138/am-2000-0116

CITATIONS
25

READS
45

5 authors, including:

Xiaoqiang Hou
Wiss, Janney, Elstner Associates, Inc.
22 PUBLICATIONS **933** CITATIONS

SEE PROFILE

Ping Yu
University of California, Davis
48 PUBLICATIONS **1,694** CITATIONS

SEE PROFILE

American Mineralogist, Volume 85, pages 173–180, 2000

^{15}N NMR study of nitrate ion structure and dynamics in hydrotalcite-like compounds

XIAOQIANG HOU,[1,*] R. JAMES KIRKPATRICK,[1] PING YU,[2] DUANE MOORE,[3] AND YEONGKYOO KIM[1,†]

[1]Department of Geology, University of Illinois at Urbana-Champaign, 1301 W. Green Street, Urbana, Illinois 61801, U.S.A.
[2]Department of Material Science and Engineering, University of Illinois at Urbana-Champaign, 1304 W. Green Street, Urbana, Illinois 61801, U.S.A.
[3]Illinois State Geological Survey, 615 E. Peabody Drive, Champaign, Illinois 61820, U.S.A.

ABSTRACT

We report here the first nuclear magnetic resonance (NMR) spectroscopic study of the dynamical and structural behavior of nitrate on the surface and in the interlayer of hydrotalcite-like compounds ($^{15}NO_3^-$-HT). Spectroscopically resolvable surface-absorbed and interlayer NO_3^- have dramatically different dynamical characteristics. The interlayer nitrate shows a well defined, temperature independent uniaxial chemical shift anisotropy (CSA) powder pattern. It is rigidly held or perhaps undergoes rotation about its threefold axis at all temperatures between –100 °C and +80 °C and relative humidities (R.H.) from 0 to 100% at room temperature. For surface nitrate, however, the dynamical behavior depends substantially on temperature and relative humidity. Analysis of the temperature and R.H. dependences of the peak width yields reorientational frequencies which increase from essentially 0 at –100 °C to 2.6×10^5 Hz at 60 °C and an activation energy of 12.6 kJ/mol. For example, for samples at R.H. = 33%, the surface nitrate is isotropically mobile at frequencies greater than 10^5 Hz at room temperature, but it becomes rigid or only rotates on its threefold axis at –100 °C. For dry samples and samples heated at 200 °C (R.H. near 0%), the surface nitrate is not isotropically averaged at room temperature. In contrast to our previous results for $^{35}Cl^-$-containing hydrotalcite ($^{35}Cl^-$-HT), no NMR detectable structural phase transition is observed for $^{15}NO_3^-$-HT. The mobility of interlayer nitrate in HT is intermediate between that of carbonate and chloride.

INTRODUCTION

Hydrotalcite is one of the few minerals with significant, permanent anion-exchange capacity, and stands in contrast to the more common clay minerals which have cation-exchange properties. Ideal hydrotalcite has a structural formula of $Mg_6Al_2(OH)_{16}CO_3 \cdot 4H_2O$ (e.g., Reichle 1986) and consists of positively charged brucite-type octahedral sheets, alternating with interlayers containing carbonate anions and water molecules. The net positive charge on the octahedral sheets is due to the partial substitution of Al for Mg. Structure refinements yield Mg and Al disordered over the octahedral sites (Bellotto et al. 1996). The actual Al/(Mg + Al) ratio varies from 0.2 to 0.45 (e.g., Titulaer et al. 1996).

Hydrotalcite-like compounds (HTs, Carrado et al. 1988) are structurally similar to hydrotalcite, but contain a wide variety of interlayer anions and 1+, 2+, 3+, and 4+ cations on the octahedral sites (e.g., Drits et al. 1987; Ulibarri et al. 1987; Ookubo et al. 1994; Titulaer et al. 1996). HTs can be synthesized either by direct co-precipitation from aqueous solution (Miyata 1975; Miyata and Okada 1977) or by exchange of interlayer anions already present in host HTs (Hansen and Taylor 1991; Reichle 1986). Products obtained from either method can be hydrothermally recrystallized to increase particle size. Hydrotalcite-like compounds have aroused increasing interest because of their ability to exchange organic and inorganic anions, and thus their potential applications in the management of hazardous chemical and radioactive waste (Abdelouas et al. 1994; Wada and Masuda 1995; Ulibarri et al. 1995; Amin and Jayson 1996; Hermosin et al. 1996; Olguin et al. 1998). As for many silicate-based clay minerals, the structural environments and dynamical behavior of the interlayer and surface species in HTs, which are most crucial to such applications, are difficult to study and poorly understood. NMR spectroscopy is an effective technique in addressing these issues due to its unique ability to simultaneously probe element-specific local structure with high resolution and to investigate atomic and molecular motion in the relevant 10^2–10^6 Hz frequency range (Kim et al. 1996; Kirkpatrick et al.1999, and references therein). For HTs, NMR has been previously used to study only $^{13}CO_3^{2-}$, $^{1,2}H_2O$, $^{35}Cl^-$, and octahedral ^{27}Al and ^{24}Mg (Marcelin et al. 1989; Dupuis et al. 1990; Mackenzie et al. 1993; van der Pol et al. 1994; Kirkpatrick et al. 1999). We present here the first ^{15}N NMR study of nitrate-containing HT with emphasis on the contrast-

*E-mail: xhou@uiuc.edu
†Current address: Korea Environment Institute, 1049-1 Sandang-Dong, Dongjak-Gu, Seoul, 156-090, Korea.

ing dynamical behavior of interlayer and surface anions. The results also show that NO_3^- has a dynamical character between the comparatively mobile ^{35}Cl (Kirkpatrick et al. 1999) and the tightly held $^{13}CO_3^{2-}$ (Miyata 1983; Van der Pol et al. 1994; Parker 1995; Chatelet et al. 1996).

Experimental methods

Two different $^{15}NO_3^-$ -HTs were synthesized by precipitation from a $Mg(NO_3)_2$. $6H_2O$ and $Al(NO_3)_3 \cdot 9H_2O$ solution (0.75 M Mg^{2+} and 0.25 M Al^{3+}, nominal Mg/Al molar ratio of 3) at 55 °C using the method of co-precipitation (Miyata 1975). After dropwise mixing, the precipitates were held in suspension at 55 °C for two hours under vigorous stirring and nitrogen flow. ^{15}N enrichment was carried out by stirring the isotopically unenriched NO_3-HT precipitates in ^{15}N enriched sodium nitrate solution ($Na^{15}NO_3$, 0.2 M) at 45 °C for 2 days. The precipitates were then centrifugally separated, washed and vacuum filtered three times to remove excess nitrate, and then dried at 70 °C for 24 hours. The samples obtained at this stage were analyzed for bulk chemical composition and investigated by powder X-ray diffraction (XRD), scanning electron microscopy (SEM) and ^{15}N NMR. An aliquot was then hydrothermally treated under autogenous pressure in a Parr vessel for 24 hours at 200 °C. The resulting suspension was again washed and vacuum filtered three times, and the precipitate was dried at 70 °C for 24 hours. The final products were again investigated by XRD, SEM, and NMR. To decrease the ^{15}N T_1 relaxation time for NMR data collection, Fe^{3+} was added to the reaction mixture during the initial preparation in molar ratios varying from 0.3% to 1.3% of the total cations.

Samples were examined using a Hitachi-S4700 scanning electron microscope at an accelerating voltage of 10 kV. For elemental analysis, the metallic elements were determined using inductively coupled plasma (ICP), and C, H, and N with a CHN analyzer. Powder XRD patterns were recorded on a Scintag diffractometer using Cu*K*α radiation, and KGa-1 kaolinite (from the Clay Minerals Repository, University of Missouri-Columbia) was added as an internal standard. NMR spectra were collected at H_0 = 11.7 T under both static and MAS conditions using a spectrometer equipped with a Techmag Aries data system, Doty Scientific MAS probe and a home built static probe. A 50.667 MHz carrier frequency was applied. The 90° pulse length was 7 ms. The recycle time used was typically 2 s, but values up to 1000 s were used to investigate T_1 relaxation effects on spectral intensity. The number of scans varied from ca. 3000 to 20 000. Solid $^{15}NH_4Cl$ was used as an external chemical shift standard, and its chemical shift was set at 37 ppm. Spectra were collected at temperatures from +80 °C to –100 °C using a liquid nitrogen cooling system and a resistance heater heating system. For spectra collected at room temperature and controlled R.H., the samples were placed in an open glass tube, equilibrated for 4 weeks over saturated salt buffers (Lide 1998), and quickly sealed in the glass tube with epoxy just before data collection. ^{15}N NMR spectra were also collected for the following samples: (1) HT mixed with D_2O to make a thick paste; (2) HT dehydrated at 200 °C in air for 2 hours, resulting in the removal of surface and interlayer water; and (3) HT dehydrated at 200 °C in air for 2 hours then rehydrated with D_2O.

Results and discusions

SEM and XRD

The two HTs prior to hydrothermal treatment are compositionally similar, except that HT-1 has higher Fe. The structural formulae based on elemental analysis are $[Mg_{0.731}Al_{0.256}Fe_{0.013}(OH)_2][(CO_3)_{0.018}(NO_3)_{0.233} \cdot nH_2O]$ for HT-1 and $[Mg_{0.745}Al_{0.252}Fe_{0.003}(OH)_2][(CO_3)_{0.025}(NO_3)_{0.205} \cdot nH_2O]$ for HT-2. The hydrothermally treated HT-2 has a structural formula essentially the same as the unrecrystallized sample, $Mg_{0.745}Al_{0.252}Fe_{0.003}(OH)_2][(CO_3)_{0.029}(NO_3)_{0.197} \cdot nH_2O]$. All samples contain considerable carbonate, even though we synthesized them under strong nitrogen flow. Microscopically, the samples are poorly dispersed and occur mostly as aggregates of circular or irregular platelets. The crystallites are typically 500 nm across and up to 30 nm thick in the recrystallized sample, but smaller and thinner in the unrecrystallized samples. Well-crystallized hexagonal platelets are also observed in the recrystallized sample.

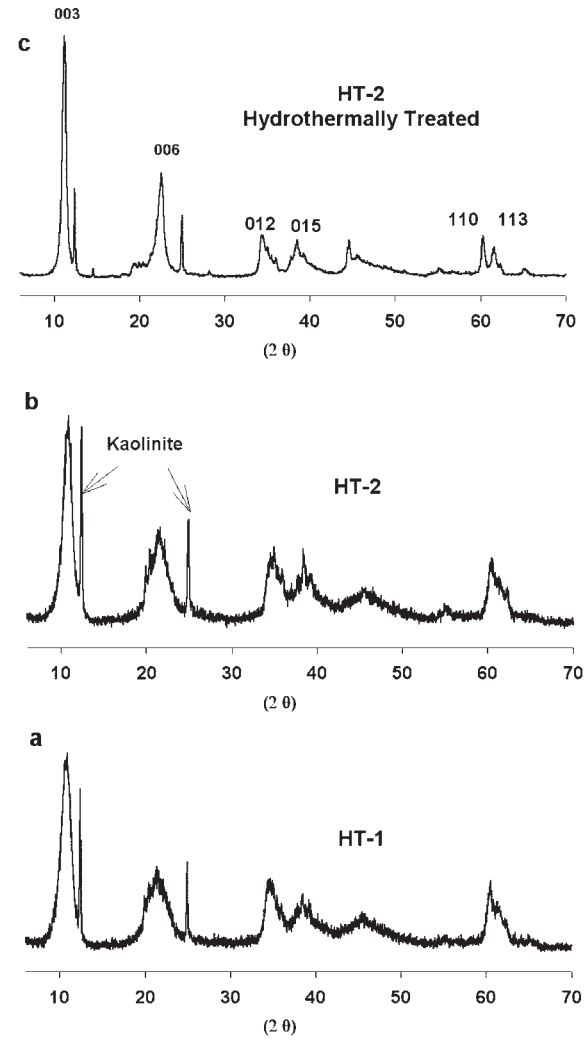

Figure 1. Powder XRD patterns for nitrate hydrotalcite-like compound (NO_3-HTs). Note peaks for KGa-1 kaolinite added as an internal standard. (**a**) HT-1 before hydrothermal treatment. (**b**) HT-2 before hydrothermal treatment. (**c**) HT-2 after hydrothermal treatment.

Random orientation powder XRD patterns (Fig. 1) show that all samples are phase pure HTs. The significant decrease in (003) peak width and increased resolution for all peaks after hydrothermal treatment indicates improved crystallinity. An approximate evaluation of crystallite thickness in the [001] direction using the Scherrer equation (Warren 1990) gives a value of ca. 9 nm for the two untreated samples and 19 nm for the hydrothermally treated sample. The (003) lattice spacings, which represent the thickness of a single structural layer, are 0.823 nm, 0.822 nm, and 0.795 nm for HT-1, HT-2, and the hydrothermally treated HT-2, respectively. All of the XRD data are comparable to those previously obtained for NO_3^--HTs prepared under similar experimental conditions (Marcelin et al. 1989).

Room temperature NMR

At room humidity and room temperature, the static ^{15}N spectrum of HT-2 (Figs. 2i and 2j) contains a sharp symmetrical peak and a broad, low asymmetrical peak. The sharp peak has a chemical shift of 374 ppm, the same as nitrate in $Na^{15}NO_3$ solution (Fig. 3b). Because ^{15}N in nitrate is always coordinated to three O atoms and the bonding of the nitrate ion to other species is highly ionic, the chemical shift does not vary much. The MAS spectrum of this sample (Fig. 2k) shows only one central peak and associated spinning side bands. Thus, under MAS the broad peak is fully averaged and had a chemical shift unresolvable from that of the narrow peak. At room temperature and variable R.H., the broad, asymmetric component is always present, and the width of the symmetrical peak narrows progressively with increasing R.H. (Figs. 2a–2f). At R.H. = 0% it is unresolvable from the broad peak. At 11% R.H., its full-width at half-height (FWHH) is 42.4 ppm, and at 100% R.H. the FWHH is 3.2 ppm. The broad (R.H. independent) peak is well simulated by a uniaxial chemical shift anisotropy (CSA; Stebbins 1988) pattern with principal components of 448 ppm, 448 ppm, and 226 ppm, yielding an isotropic chemical shift of 374 ppm, the same as the maxima of the sharp peaks in the static spectra and in the MAS spectrum. This is the pattern expected for rigid NO_3^- such as that in crystalline $Na^{15}NO_3$ (Fig. 3a). ^{15}N has spin $I = 1/2$, and thus CSA is expected to dominate the static line shape of rigidly held sites. The peaks should narrow substantially under MAS and by isotropic molecular motion at frequencies larger than ca. 10 kHz, as in $Na^{15}NO_3$ solution (Fig. 3b). Thus, the narrow peak is readily interpreted as due to nitrate undergoing isotropic dynamical averaging. The static spectrum of the sample heated at 200 °C (Fig. 2g) is essentially the same as at R.H. = 0 (Fig. 2a), but it has sharper features. Rehydration of the heated sample with D_2O (Fig. 2h) causes the sharp peak to return, but the broad one remains unchanged. Based on thermal gravimetric analysis (TGA) data (not shown), NO_3-HT loses all of its surface and interlayer water by 200 °C. Sample HT-1 gives spectra similar to HT-2 except that they are slightly broader because of the higher iron content (spectra not shown).

The ^{15}N NMR spectra of the recrystallized samples contain the same peaks (Fig. 4). The line shape of the broad component is again well simulated by the CSA pattern with principal components of 448 ppm, 448 ppm, and 226 ppm as for unrecrystallized sample, and there is a narrower symmetrical peak at 374 ppm. At a recycle time of 2 s, the relative intensity (peak area) of the broad peak increases from 10% for the unrecrystallized sample to 62% for the recrystallized one.

Accurate quantitation of the atomic ratio of the two sites is not possible in this study because of the long ^{15}N spin-lattice relaxation time T_1 (Saluvere and Lippmaa 1970). The dominant mechanism for ^{15}N relaxation in our HTs is probably the interaction between ^{15}N and the unpaired electrons of Fe^{3+} paramagnetic centers (so-called paramagnetic relaxation), although other mechanisms including the ^1H-^{15}N dipolar interaction and ^{15}N CSA probably contribute. Not all individual ^{15}N nuclei are affected equally by these mechanisms. Some nitrates are closer to the paramagnetic centers than others, and the e^--^{15}N relaxation rate, T_1^{-1}, is proportional to r^{-6}, where r is the distance between ^{15}N and Fe^{3+} (Martin et al. 1981). In experiments with variable recycle time, the intensity ratio of the broad to narrow peaks for the recrystallized sample changes from 1.6 at a recycle time of 2 s to 2.2 at 60 s, and to 3.2 at 603 s. Clearly, the narrow peak has a shorter T_1 relaxation time than the broad peak, and even at the prohibitingly long recycle time of 1000 s, peak areas probably underestimate the abundance of the broad peak. Static ^{15}N NMR spectra for a sample containing well separated solid $Na^{15}NO_3$ and $Na^{15}NO_3$ solution with a ^{15}N atomic solid/solution ratio of 3.7 yield broad/sharp peak area ratio of only 2.1, even at a recycle time of 1003 s. Thus, ^{15}N in solid $Na^{15}NO_3$ is not fully relaxed even at this long recycle time, confirming that ^{15}N T_1 values are a routine problem for solids. The peak widths and positions, however, do not vary with recycle time, allowing interpretation to be based on them. Despite the lack of quantitative peak areas, the increase in relative abundance of the broad peak at a recycle time of 2 s after recrystallization indicates that it represents interlayer nitrate, and that the narrow peak represents surface nitrate. The assignment is similar to that for surface and interlayer ^{35}Cl in hydrocalumite (Kirkpatrick et al. 1999), except that for hydrocalumite the peak due to interlayer Cl is broad due to unaveraged second-order quadrupolar interaction rather than CSA. Crystallite growth during hydrothermal treatment leads to decreased surface area as demonstrated by both XRD and SEM. Both surface and interlayer $^{15}NO_3^-$ are expected to be observable because of the large surface area of the HT samples (e.g., Titulaer et al. 1996)

Several lines of evidence strongly support this interpretation. $^{15}NO_3$-HTs quickly washed with natural isotopic abundance $NaNO_3$ and NaCl solutions (exposure time less than 10 s) yield greatly reduced intensity for the surface sites. Such washing should exchange surface nitrate but not significantly affect interlayer nitrate. This is because exchange of the interlayer sites requires long-range diffusion, and the Coulombic potential in the interlayer is larger than on the surface. In addition, surface nitrate should have a shorter T_1 value than interlayer nitrate because faster reorientational motion should lead to increased relaxation via CSA and possibly ^{15}N-^1H dipolar interactions. Thus its signal should be enhanced at short recycle times, as observed. The decreasing peak width with increasing R.H. (Fig. 2) is also consistent with this interpretation and demonstrates the different dynamical behavior of surface and interlayer nitrate. Because of its uniaxial symmetry,

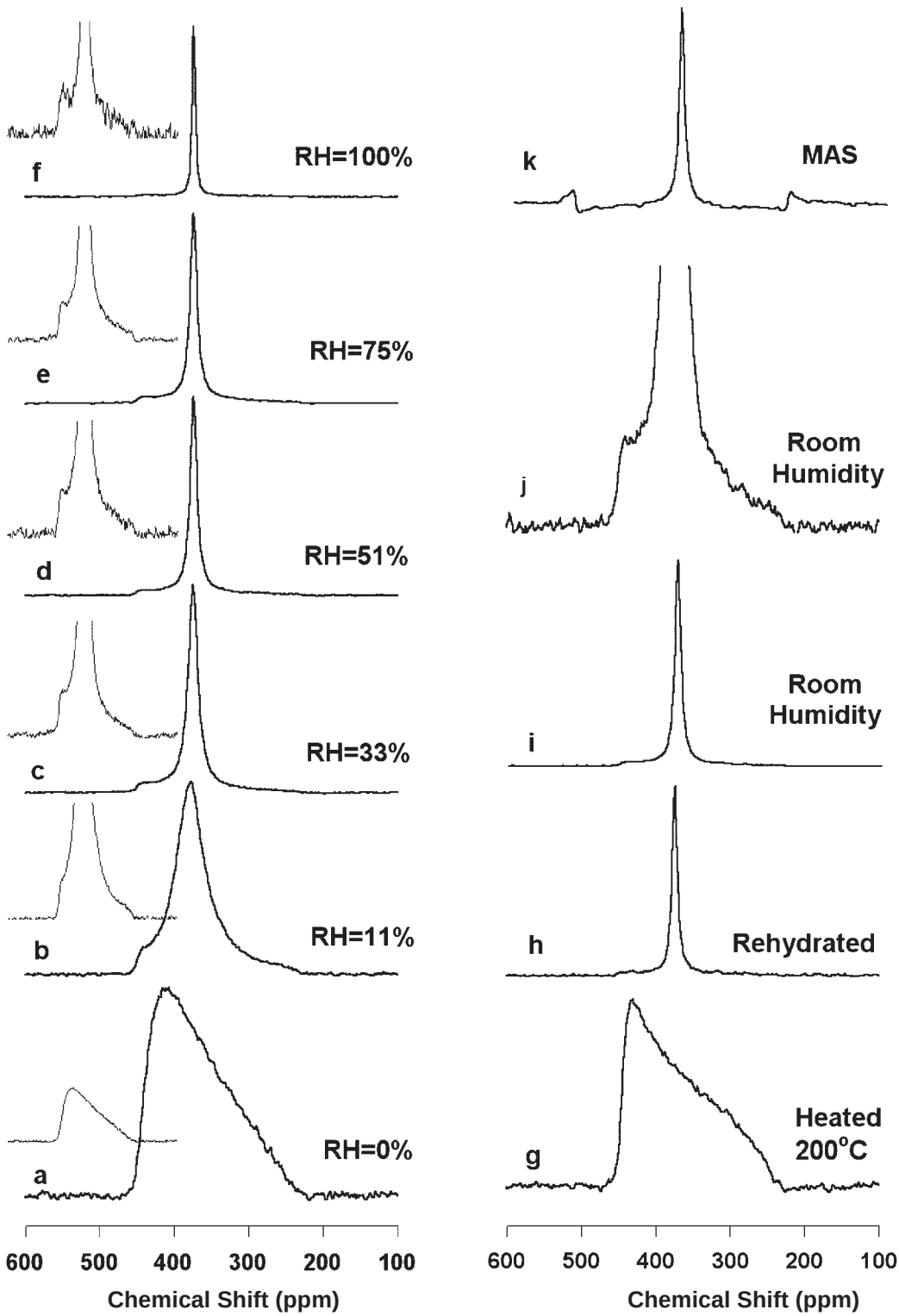

FIGURE 2. ^{15}N NMR spectra for nitrate hydrotalcite-like compounds (HT-2) under different relative humidities (RH) and treatments. Spectrum h is the heated sample re-saturated with D_2O. Spectrum j is the same as i but much expanded in vertical scale to highlight the broad component. All spectra were collected under static conditions and room temperature except k, which is a magic angle spinning (MAS) spectrum at room temperature. Inset spectra in a–f are normalized to the height of the broad component.

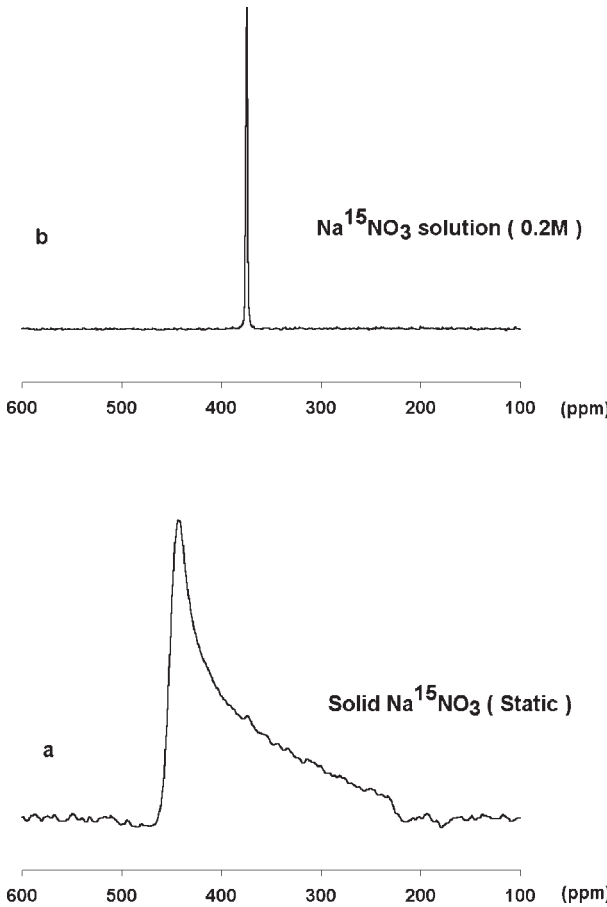

FIGURE 3. ^{15}N NMR spectra for solid $Na^{15}NO_3$ (**a**) and $Na^{15}NO_3$ solution (**b**).

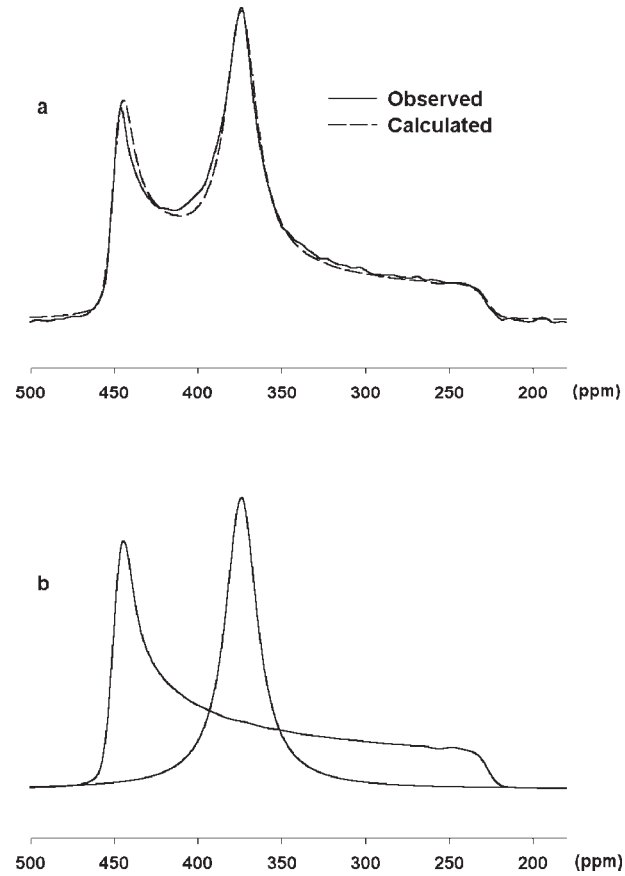

FIGURE 4. ^{15}N NMR spectra for recrystallized HT-2 at room temperature and room humidity. (**a**) Observed and calculated spectra. The calculated line is the sum of two components in b. (**b**) Calculated components used in fitting the observed spectra.

rigidly held nitrate exhibits a well defined CSA powder pattern (Fig. 4a). The only way for a sample to yield a narrow isotropic peak in a static spectrum is for the nitrate to be undergoing isotropic reorientation at a frequency greater than ca. 10 times of rigid peak width, here ca. 10^5 Hz. The observed decreasing peak width with increasing R.H. for this component is expected for surface nitrate as the amount of surface water increases. In contrast, changing R.H. has little effect on the interlayer spacing (Martin and Pinnavaia 1986), indicating that the local structural environment of the interlayer nitrate does not change, and consistent with the assignment of the R.H. independent CSA dominated line shape to interlayer nitrate. We have assigned the CSA pattern for interlayer nitrate to rigidly held sites, but in fact, both rigid nitrate and nitrate rotating rapidly on its threefold axis would yield the same CSA pattern. In both cases the symmetry is axial, and NMR line shape analysis cannot distinguish the two possibilities. There is no evidence that the interlayer nitrate is not rigidly held, but variable temperature ^{17}O NMR of nitrate would distinguish these two possibilities. Based on the current data it is not possible to distinguish surface nitrate held on planar sites (external basal surface) and edge sites (broken edges of sheets), which can be very different for montmorillonite and illite (Keren and O'Connor 1982). This is because the ranges of isotropic ^{15}N chemical shifts and static CSA values are small due to the invariant structure of the anion. This situation also contrasts with previously observed ^{133}Cs NMR results for Cs on illite, for which broken edge and basal planar surface sites can be distinguished (Kim et al. 1996). The average particle diameter of about 500 nm and thickness of about 20–30 nm inferred from the XRD and SEM observations described above suggest that most of the exposed surface in our samples occurs on basal surfaces.

Variable temperature NMR and surface nitrate dynamics

Variable temperature static ^{15}N NMR spectra collected at room humidity for the recrystallized HT-2 sample (Fig. 5) further confirm these interpretations and provide significant insight into the dynamical behavior of the surface nitrate. The line shape of the broad component remains essentially unchanged at all temperatures examined, again indicating that the interlayer nitrate is rigidly held or rotates around only on its threefold axis. The peak width of the component due to the

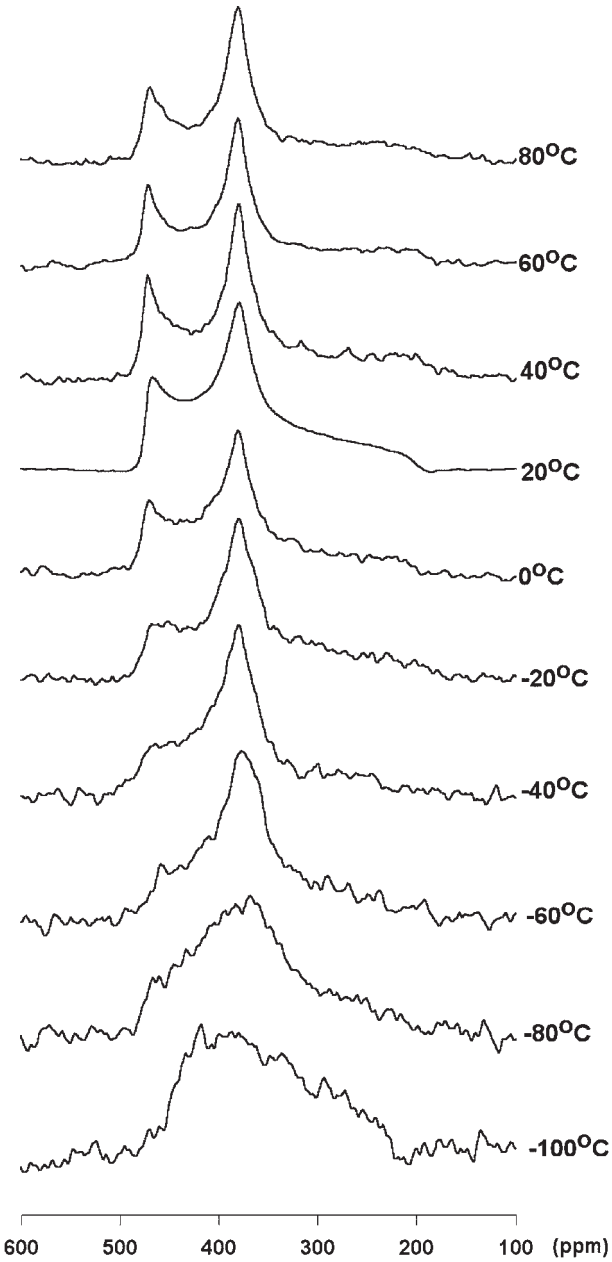

FIGURE 5. Static ^{15}N NMR spectra of recrystallized HT-2 at room humidity and the indicated temperature.

surface nitrate increases with decreasing temperature, indicating a decreasing frequency of reorientational motion with decreasing temperature. At –100 °C, this component shows a broad CSA pattern and is unresolvable from the component due to interlayer nitrate, although the signal to noise ratio is poor. Thus, at –100 °C random reorientation on the kHz time scale has essentially stopped. The reorientation rate of the surface nitrate can be estimated from the temperature dependence of its NMR peak width (Gutowsky and Pake 1950; Moroz et al. 1998). The experimental line width β (FWHH) obeys the following equation:

$$(\beta^2-\beta_h^2) / (\beta_l^2-\beta_h^2) = 2/\pi \arctan (\beta/\nu_c) \quad (1)$$

where β_h and β_l are the smaller and larger limits for β, and ν_c is the reorientational frequency (1/correlation time), which varies with temperature as

$$\nu_c = \nu_0 \exp(-E_a/k\,T) \quad (2)$$

We take β_h to be 25 ppm (FWHH at 80 °C), and β_l to be the static peak width, 234 ppm. The reorientation frequency ν_c at each temperature can be obtained from Equation 1 (Fig. 6). The fit of ν_c to Equation 2 yields an apparent activation energy E_a of 12.6 kJ/mol and a ν_0 of 2.1×10^7 Hz (or $\tau = 1/\nu_0 = 4.7 \times 10^{-8}$ s). This apparent activation energy is in the range expected for processes controlled by hydrogen bonding (Jonas and Brown 1982; Kalinichev and Bass 1997). Jonas and Brown (1982) investigated the dynamical behavior of water in kaolinite-water suspensions using ^{1}H and ^{2}D NMR. Their reported activation energy for reorientation of water molecules on the kaolinite surface is 4.6 kJ/mol, which is much lower than the corresponding value of 21.3 kJ/mol for bulk water. Dupuis et al. (1990) reported E_a = 9.6 kJ/mol and $\nu_0 = 1.2 \times 10^8$ Hz for water in HT. Our nitrate activation energy is comparable but higher, perhaps due to the larger size of nitrate and its negative charge, which causes Coulombic attraction to the hydroxide layers, in addition to hydrogen bonding. The reduced ν_0 for nitrate compared to water on HT is again probably due to Coulombic interactions. Similarly, Equation 1 can be applied to the variable humidity ^{15}N NMR data in Figure 2 to derive reorientational frequencies at room temperature and variable R.H. Here the correct β_h is the $Na^{15}NO_3$ solution peak width of 0.89 ppm because at 100% R.H. the humidity condition is essentially bulk solution. β_l remains the static peak width of 234 ppm. The calculated ν_c values increase progressively with increasing R.H. from essentially zero at R.H. = 0% to ca. 4.2×10^4 Hz at R.H. = 11%, to 6×10^5 Hz at R.H. = 100% (Fig. 7). The trend of

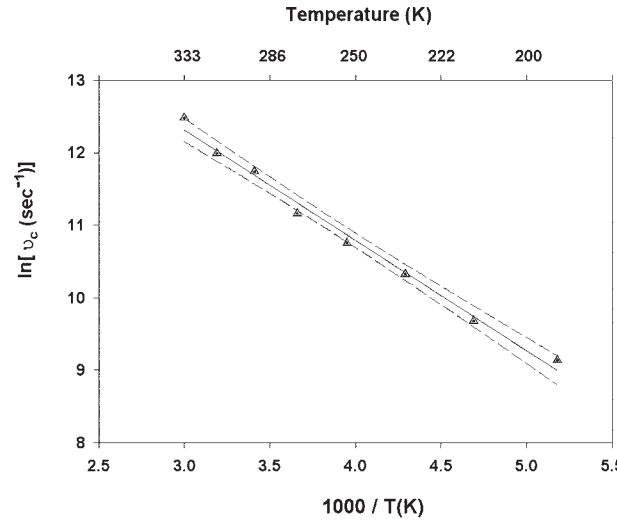

FIGURE 6. Temperature dependence of the reorientation frequency of the surface nitrate. Analytical precision is less for the reorientational frequency than the symbol size.

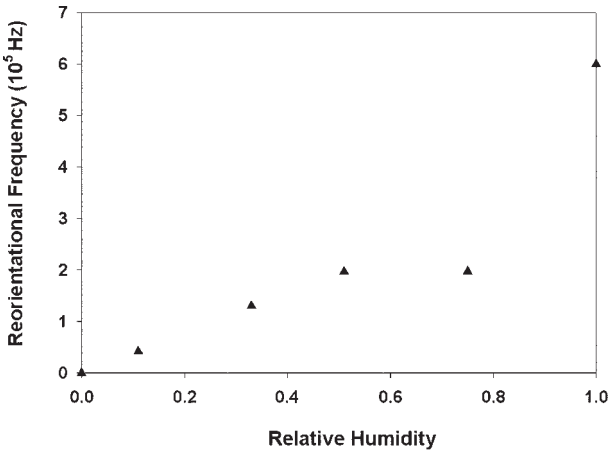

FIGURE 7. Relative humidity dependence of the reorientation frequency of the surface nitrate. Analytical precision is less for the reorientational frequency than the symbol size.

increasing ν_c at low R.H., less variation at intermediate values, and a large increase at high R.H. parallels the variation in amount of adsorbed water commonly observed for oxide materials (Parks 1990). For instance, for quartz there is one statistical monolayer at R.H. = 10%, at about 80% 5 layers, and at 100% about 50 layers (Parks 1990). Similar variation occurs for other materials and is expected for HTs. At R.H. near 0%, little surface water is present, and nitrate is probably strongly hydrogen-bonded to surface OH^- groups as inner-sphere complexes. At R.H. = 11%, the presence of some surface water decreases the relative importance of NO_3^--OH^- hydrogen bonding and increases the probability of NO_3^- motion such that its reorientational frequency is in the kHz range. Higher R.H. leads to more surface water and progressively less hydrogen bonding to the OH^- groups, making the nitrate even more mobile. At 100% R.H., the surface nitrate is probably present dominantly as outer sphere complexes and behaves almost the same as in bulk water. Although surface NO_3^- is isotropically mobile when water is present, it cannot be washed away with deionized water. It is required for charge balance and Coulombic interaction keeps it attracted to the surface.

The mobility of interlayer nitrate in HT is intermediate between that of carbonate and chloride. The ^{13}C NMR spectra of Van der Pol et al. (1994) indicate that carbonate is rigidly held. They proposed that it is hydrogen bonded to the OH groups of the main layer and that the C_2 symmetry axes of water and the C_3 axes of carbonate are perpendicular to the layer. We believe that this is also true for nitrate HTs, although the nitrate may be undergoing rapid threefold rotation. However, interlayer nitrate can be readily exchanged for anions such as Cl^-, SeO_3^{2-} and SeO_4^{2-}, whereas interlayer carbonate cannot be easily substituted by these anions (e.g., Miyata 1983; Parker et al. 1995; Hou et al. 1998). We attribute this different behavior to the difference in charge and ionic radius between nitrate and carbonate. Carbonate is divalent and is smaller than nitrate. Thus its Coulombic attraction to the main layer is greater, increasing the strength with which it is held. ^{35}Cl NMR spectra for hydrotalcite show that interlayer Cl^- is mobile, with an increasing reorientational frequency with increasing temperature at temperatures above –80 °C (Kirkpatrick et al. 1999). This motion averages the local electric field gradient and thus decreases the apparent quadrupole coupling constant. A poorly defined structural phase transition occurs for Cl-HT over the temperature interval from –97 °C to –40 °C. In contrast, isotropic reorientation of interlayer nitrate is not observed. This is probably a steric effect due to the non-spherical shape of the nitrate, but greater hydrogen bonding to the three O atoms may contribute.

ACKNOWLEDGMENTS

This research is supported by the NSF grant no. EAR 95-26317. We thank Andrey Kalinichev and Jianwei Wang for useful discussion. We also thank the two anonymous reviewers for detailed comments and improvement of the manuscript.

REFERENCES CITED

Abdelouas, A., Crovissier, J.L., Lutze, W., Fritz, B., Mosser, A., and Muller, R. (1994) Formation of hydrotalcite-like compounds during R7T7 nuclear waste glass and basaltic glass alteration. Clays and Clay Minerals, 42, 526–533.

Amin, S. and Jayson, G.G. (1996) Humic substance uptake by hydrotalcites and PILCS. Water Resources, 30, 299–306.

Bellotto, M., Rebours, B., Clause, O., Lynch, J., Bazin, D., and Elkaiem, E. (1996) A reexamination of hydrotalcite crystal chemistry. Journal of Physical Chemistry, 100, 8527–8534.

Carrado, K.A., Kostapapas, A., and Suib, S.L. (1988) Layered double hydroxides (LDHs). Solid State Ionics, 26, 77–86.

Drits, V.A., Sokolova, T.N., Sokolova, G.V., and Cherkashin, V.I. (1987) New members of the hydrotalcite-manasseite group. Clays and Clay Minerals, 35, 401–417.

Dupuis, J., Battut, J.P., Fawal, Z., and Hajjimohamad, H. (1990) Nuclear magnetic resonance analysis of protons in the hydrotalcite type compound $Zn_{2/3}Al_{1/3}(OH)Cl_{1/3}\cdot nH_2O$. Solid State ionics, 42, 251–255.

Gutowsky, H.S. and Pake, G.E. (1950) Structural investigation by means of nuclear magnetism. II. Hindered rotation in solids. Journal of Chemical Physics, 18, 162–170.

Hansen, H.C.B. and Taylor, R.M. (1991) The use of glycerol intercalates in the exchange of CO_3^{2-} with SO_4^{2-}, NO_3^- or Cl^- in pyroaurite-type compounds. Clay Minerals, 26, 311–327.

Hermosin, M.C., Pavlovic, I., Ulibarri, M.A., and Cornejo, J. (1996) Hydrotalcite as sorbent for trinitrophenol: sorption capacity and mechanism. Water Resources, 30, 171–177.

Hou, X-Q., Kirkpatrick, R.J., and Kim, Y. (1998) ^{77}Se NMR investigation of SeO_4^{2-} and SeO_3^{2-} hydrotalcite-like compounds (HTs) (Abstract). 17th General Meeting of the International Mineralogical Association, Toronto, Canada.

Jonas, J. and Brown, D. (1982) NMR study of kaolinite-water system at high pressure. Journal of Colloid and Interface Science, 89, 374–378.

Kalinichev, A.G. and Bass, J.D. (1997) Hydrogen bonding in supercritical water. 2. Computer simulations. Journal of Physical Chemistry A, 101, 9720–9727.

Keren, R. and O'Connor, G.A. (1982) Effect of exchange ions and ionic strength on boron adsorption by montmorillonite and illite. Clays and Clay Minerals, 30, 341–346.

Kim, Y., Kirkpatrick, R.J., and Cygan, R.T. (1996) ^{133}Cs NMR study of cesium on the surfaces of kaolinite and illite. Geochemica et Cosmochimica Acta, 60, 4059–4074.

Kirkpatrick, R.J., Ping, Y., Hou, X., and Kim, Y. (1999) Interlayer structure, anion dynamics, and phase transitions in mixed-metal layered hydroxides: variable temperature ^{35}Cl NMR spectroscopy of hydrotalcite and Ca-aluminate hydrate (hydrocalumite). American Mineralogist, 84, 1186-1190.

Levy, G.C. and Lichter, R.L., Eds. (1979) Nitrogen-^{15}Nuclear Magnetic Resonance Spectroscopy. Wiley, New York.

Lide, D.R. (1998) CRC Handbook of Chemistry and Physics (79th Edition), 15–25, CRD Press, Boca Raton, Florida.

MacKenzie, K.J.D., Meinhold, R.H., Sherriff, B.L., and Xu, Z. (1993) ^{27}Al and ^{25}Mg solid-state magic-angle spinning nuclear magnetic resonance study of hydrotalcite and its thermal decomposition sequence. Journal of Materials Chemistry, 3, 1263–1269.

Marcelin, G., Stockhausen, N.J., Post, J.F.M., and Schutz, A. (1989) Dynamics and ordering of interlayered water in layered metal hydroxides. Journal of Physical Chemistry, 93, 4646–4650.

Martin, G.J., Martin M.L., and Gouesnard J-P. (1981) ^{15}N-NMR Spectroscopy. 10 p. Springer-Verlag, Berlin.

Martin, K.J. and Pinnavaia, T.J. (1986) Layered double hydroxides as supported anionic reagents. Halide ion reactivity in $[Zn_2Cr(OH)_6]X\cdot nH_2O$. Journal of the American Chemical Society, 108, 541–542.

Miyata, S. (1975) The synthesis of hydrotalcite-like compounds and their structures and physico-chemical properties-I. Clays and Clay Minerals, 23, 369–375.

———(1983) Anion-exchange properties of hydrotalcite-like compounds. Clays and Clay Minerals, 31, 305–311.

Miyata, S., and Okada, A. (1977) Synthesis of hydrotalcite-like compounds and their physico-chemical properties—The systems Mg^{2+}-Al^{3+}-SO_4^{2-} and Mg^{2+}-Al^{3+}-CrO_4^{2-}. Clays and Clay Minerals, 25, 14–18.

Moroz, N.K., Afanassyev, I.S., Fursenko, B.A., and Belitsky, I.A. (1998) Ion mobility and dynamic disordering of water in analcime. Physics and Chemistry of Minerals, 25, 282–287.

Olguin, M.T., Bosch, P., Acosta, D., and Bulbulian, S. (1998) ^{131}I sorption by thermally treated hydrotalcites. Clays and Clay Minerals, 46, 567–573.

Ookubo, A., Ooi, K., Tani F., and Hayashi, H. (1994) Phase transition of Cl-intercalated hydrotalcite-like compounds during ion exchange with phosphates. Langmuir, 10, 407–411.

Parker, L.M., Milestone, N.B., and Newman, R.H. (1995) The use of hydrotalcite as an anion absorbent. Industrial and Engineering Chemistry Research, 34, 1196–1202.

Parks, G.A. (1990) Surface energy and adsorption at mineral-water interfaces: an introduction. In Mineralogical Society of America Reviews in Mineralogy, 23, 133–175.

Reichle, W.T. (1986) Synthesis of anionic clay minerals (mixed metal hydroxides, hydrotalcite). Solid State Ionics, 22, 135–141.

Saluvere, T. and Lippmaa, E. (1970) Spin-lattice relaxation of ^{15}N nuclei. Chemical Physics Letters, 7, 545–548.

Stebbins, J.F. (1988) NMR spectroscopy and dynamic processes in mineralogy and geochemistry. In Mineralogical Society of America Reviews in Mineralogy, 18, 405–429.

Titulaer, M.K., Talsma, H., Jansen, J.B.H., and Geus, J.W. (1996) The formation of ice between hydrotalcite particles measured by thermoporometry. Clay Minerals, 31, 263–277.

Ulibarri, M.A., Cornejo, J., and Hernadez, M.J. (1987) Effects of hydrothermal treatment on textural properties of $[Al_2Li(OH)]_2CO_3 \cdot nH_2O$. Journal of Materials Science, 22, 1168–1172.

Ulibarri, M.A., Pavlovic, I., Hermosin, M.C., and Cornejo, J. (1995) Hydrotalcite-like compounds as potential sorbents of phenols from water. Applied Clay Sciences, 10, 131–145.

van der Pol, A., Mojet, B.L., van de Ven, E., and de Boer, E. (1994) Ordering of intercalated water and carbonate anions in hydrotalcite-An NMR study. Journal of Physical Chemistry, 98, 4050–4054.

Wada, S-I. and Masuda, K. (1995) Control of salt concentration of soil solution by the addition of synthetic hydrotalcite. Soil Science and Plant Nutrition, 41, 377–381.

Warren, B.L., Ed. (1990) X-ray diffraction, 253 p. Dover Publications, Inc., New York.

MANUSCRIPT RECEIVED APRIL 12, 1999
MANUSCRIPT ACCEPTED AUGUST 5, 1999
PAPER HANDLED BY JONATHAN F. STEBBINS